Engineering and Technology Journal
Journal homepage: engtechjournal.org

Nonlinear Finite Element Analysis of High Strength Fiber Reinforced Concrete Beams

Zinah A. Abdul Hussein[a*]

[a] Civil Engineering Department, University of Technology, Baghdad, Iraq. 40187@uotechnology.edu.iq

[*] Corresponding Author.

Submitted: 23/01/2008 Accepted: 14/12/2008 Published: 25/09/2020

K E Y W O R D S

Beams, Fiber , Finite Element ,Nonlinear

A B S T R A C T

This research work presents a nonlinear finite element investigation on the behavior of high strength fiber reinforced concrete beams. This investigation is carried out in order to get a better understanding of their behavior throughout the entire loading history. The three- dimensional 20-node brick elements are used to model the concrete, while the reinforcing bars are modeled as axial members embedded within the concrete brick elements. The compressive behavior of concrete is simulated by an elastic-plastic work-hardening model followed by a perfectly plastic response, which terminate at the onset of crushing. In tension, a fixed smeared crack model has been used.

How to cite this article: Z. A. Abdul Hussein, "Nonlinear Finite Element Analysis of High Strength Fiber Reinforced Concrete Beams," Engineering and Technology Journal, Vol. 38, Part A, No. 09, pp. 1293-1304, 2020.
DOI: https://doi.org/10.30684/etj.v38i9A.1840

1. INTRODUCTION

In recent years, the use of high strength concrete has increased rapidly as a result of the demand for higher strength, relatively lighter weight, and durable concrete. The major difference between the normal strength concrete and high strength concrete is that the high strength concrete tends to behave as elastic and more brittle material compared with normal strength concrete [1]. The observed inverse relationship between strength and ductility is a serious drawback if the use of high strength concrete is to be considered in some structural applications. However, such a drawback can be over came by addition of strong discontinuous fibers. It can be safely said today that one of the most desirable benefits of adding fibers to concrete is to increase its energy absorbing capability, ductility and toughness as often characterized by the shape of the area under the post-peak portion of its stress-strain curve [2]. The choice of the panels or membrane elements was intended to isolate the effect of other un preferred combination of stresses, and focus on the reduction of concrete compressive strength in the presence of transverse tensile straining of reinforcement on what is called softening phenomenon.

2. FINITE ELEMENT MODEL

In the present research work, a full three - dimensional finite element idealization has been used. This idealization gives accurate simulation for geometry, type of failure and location of reinforcing bars the 20-node quadratic brick element shown in Figure 1 Is adopted to represent concrete in the present study.

The reinforcement representation that is used in this study is the embedded representation, Figure1. The reinforcing bar is considered to be an axial member built into the concrete element. The reinforcing bars were assumed to be capable of transmitting axial force only.

The numerical integration is generally carried out using the 27 (3x3x3) point Gaussian type integration rules.

The nonlinear equations of equilibrium have been solved using an incremental-iterative technique operating under load control. The nonlinear solution algorithm that is used in this research work is the modified Newton –Raphson method in which the stiffness matrix is updated at the 2nd, 12th, 22nd, etc. iterations of each increment of loading.

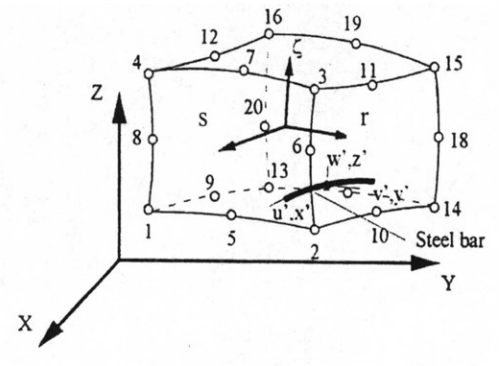

Figure 1: The twenty-node brick element.

3. MATERIAL MODEL ADOPTED IN THE ANALYSIS

I. Behavior in Compression

In compression, the behavior of concrete is simulated by an elastic-plastic work hardening model followed by a perfectly plastic response, which is terminated at the onset of crushing. The growth of subsequent loading surfaces is described by an isotropic hardening rule. A parabolic equivalent uniaxial stress-strain curve has been used to represent the work hardening stage of behavior and the plastic straining is controlled by an associated flow rule.

The concrete strength under multidimensional state of stress is a function of the state of stress and cannot be predicted by simple tensile, compressive and shearing stress independent of each other. So the state of stress must be scaled by an appropriate yield criterion to convert it to equivalent stress that could be obtained from simple experimental test. The yield criterion that has been used successfully by many investigators [3, 4] can be expressed as

$$f(\{\sigma\}) = (\alpha I_1 + 3\beta J_2)^{0.5} = \sigma_0 \qquad (1)$$

Where α and β are material parameters which are dependent on the type of concrete, mainly on the volume fraction of fiberV_f, and their values are shown in Table I [5, 6].

I_1 is the first stress invariant and J_2 is the second deviator stress invariant. σ_0 is an equivalent effective stress at the onset of plastic deformation which can be determined from a uniaxial compression test.

In a reinforced concrete member, a significant degradation in compressive strength can result due to the presence of transverse tensile straining after cracking. In the present study, Vecchio et al. models are used for HSC [7] members, which illustrates the use of the reduction factor, λ. The compressive reduction factor, λ, for HSC is given as:

$$\lambda = \frac{1}{1+K_c . K_f} \quad (2)$$

Where K_c is a factor representing the effect of the transverse cracking and straining and K_f is a factor representing the effect of concrete compressive strength f'_c.

$$K_c = 0.35(\frac{\varepsilon_1}{\varepsilon_3} - 0.28)^{0.8} \quad (3)$$

and

$$K_f = 0.1825\sqrt{f'_c} \geq 1.0 \quad (4)$$

Where ε_1 is the tensile strain in the direction normal to the crack and ε_3 is the compressive strain in the direction parallel to the crack.

TABLE I: Material parameters.

V_f	α	β
0.0	$0.3546798\sigma_o$	1.3546798
0.5	$1.0993042\sigma_o$	2.0993042
1.0	$1.4960526\sigma_o$	2.4900526
1.5	$1.7960526\sigma_o$	2.7960526

II. Behavior in Tension

In tension, linear elastic behavior prior to cracking is assumed. Cracking is governed by the attainment of a maximum principal stress criterion. A smeared crack model with fixed orthogonal cracks is assumed to represent the cracked sampling point. The post-cracking tensile stress-strain relations, Figure 2, [8, 9] and the reduction in shear modulus with increasing tensile strain Figure 3, [10] have been adopted in the present work. The tensile strain at peak tensile stress (ε_{tf1}) is given by:

$$\varepsilon_{tf1} = \varepsilon_1(1 + 0.35N_f . d_f . L_f) \quad (5)$$

Where N_f is the number of fiber per unit area; given by:

$$N_f = \eta_0[\frac{4V_f}{\pi\, d'_f}] \quad (6)$$

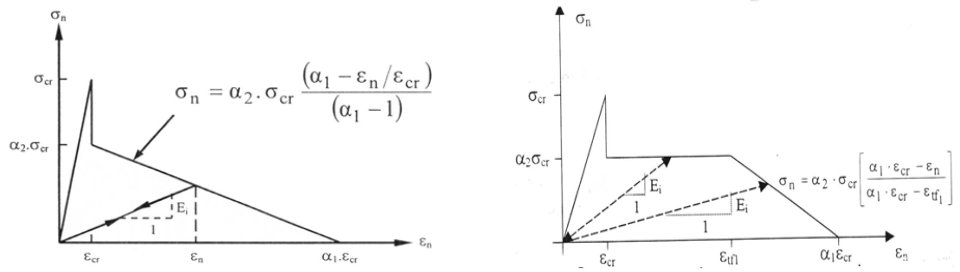

a) Plain concrete. b) Fiber reinforced concrete.

Figure 2: Post-cracking models for cracked concrete.

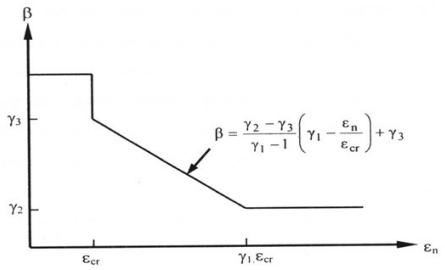

Figure 3: Shear retention model for cracked concrete.

III. Behavior of Steel Fiber Reinforced Concrete

In compression, an empirical equation for peak strain value in uniaxial compression of high strength fiber reinforced concrete ε_{pf} suggested by AL- AZZAWI [11] is adopted in the present study as:

$$\varepsilon_{pf} = 0.00212 + 0.001V_f * L_f/d_f \quad (7)$$

In his study, an empirical equations for (f'_{cf}) suggested by Bunni [12] is adopted and is given by:

$$f'_{cf} = (f'_c)^{0.941}.(V_f L_f/d_f)^{0.054} \quad (8)$$

According to test results reported in reference [13] the concrete peak value of the tensile stress of high strength fiber reinforced concrete (f'_{tf}) is proposed in terms of compressive strength of reinforce (f'_c) and fiber volume fraction (V_f in percent) as follows:

$$f_{tf} = 058\sqrt{f'_c} + 302V_f \quad (9)$$

4. NUMERICAL EXAMPLE

I. Description of Test Specimens

A total of 8 reinforced concrete beams were tested by Ashour and Wafa [14] under monotonic loading up to failure. In order to check the validity of the present material model, these beams were chosen for this research work to carry out the finite element analysis. These beams were B4-0, B4-0.5, B4-1.0, B4-1.5, B6-0, B6-0.5, B6-1.0 and B6-1.5 .All tested beams had a longitudinal steel ratio of 1.39% and shear –span/depth (a/d) ratio of 4 and 6. All beams failed in flexure mode. Figure 4 shows the loading arrangement and reinforcement details. Dimension and reinforcement details for Ashour and Wafa beams are listed in Table II.

TABLE II: Dimension and reinforcement details for Ashour and Wafa beams.

No.	*Beam Designation*	V_f *(%)*	*a mm*	*L mm*	*a/ d*	*As* mm^2	*Aś* mm^2	ρ_w *(%)*	ρ_v *(%)*	*S mm*	*Cross Section Type*
1	B-4-0.0	0.0	1060	2620	4	628	56.5	1.39	0.39	150	B-B
2	B-4-0.5	0.5	1060	2620	4	628	56.5	1.39	0.39	150	B-B
3	B-4-1.0	1.0	1060	2620	4	628	56.5	1.39	0.39	150	B-B
4	B-4-1.5	1.5	1060	2620	4	628	56.5	1.39	0.39	150	B-B
5	B-6-0.0	0.0	1590	3680	6	628	56.5	1.39	0.39	150	B-B
6	B-6-0.5	0.5	1590	3680	6	628	56.5	1.39	0.39	150	B-B
7	B-6-1.0	1.0	1590	3680	6	628	56.5	1.39	0.39	150	B-B
8	B-6-1.5	1.5	1590	3680	6	628	56.5	1.39	0.39	150	B-B

The same type of fibers was used throughout the test program. The fibers were hooked, 60mm in length and 0.8mm in diameter making an aspect ratio (L_f/d_f) of 75 . The steel fibers had an ultimate tensile strength of 1100MPa.

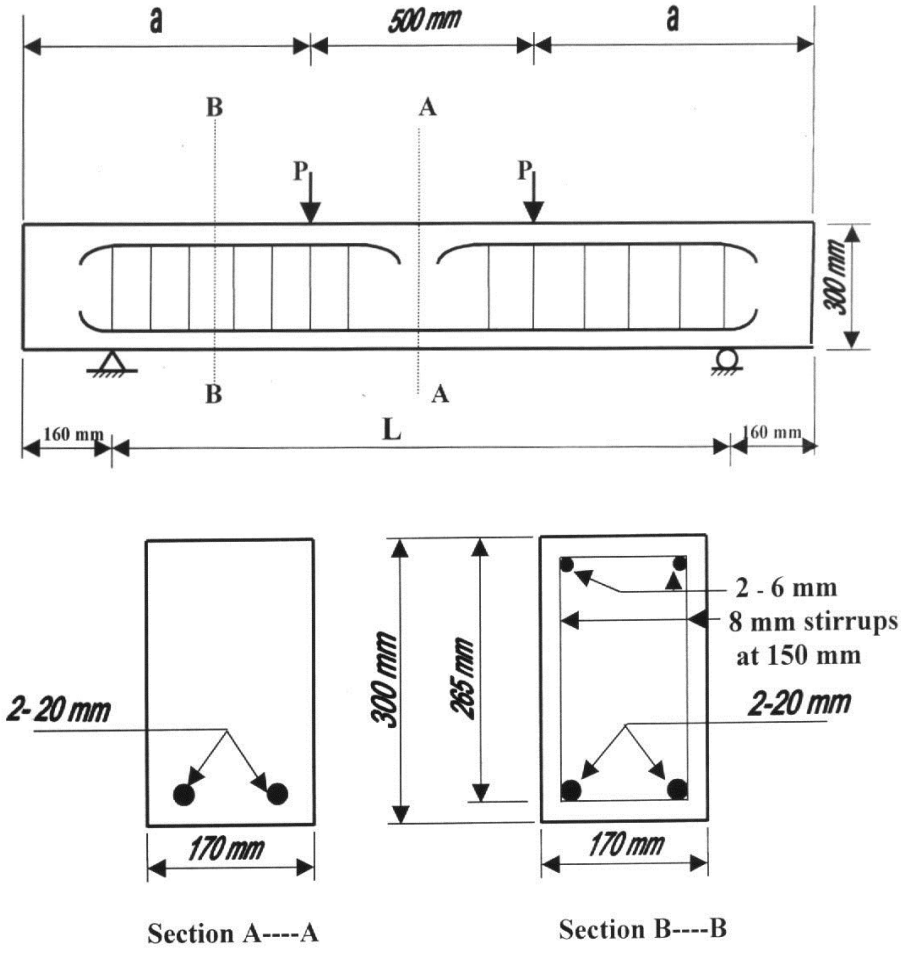

Figure 4: Dimensions and reinforcement details for Ashour and Wafa beams.

II. Finite Element Idealization and Material Properties

By making use of the symmetry of loading, geometry and reinforcement distribution of the tested beams, only one quarter of the beam will be considered in the numerical analyses. In the present study, the chosen segments were modeled using 4 brick elements. The finite element mesh, boundary conditions, and loading arrangement are shown in Figure 5 .The dimensions, material properties and the additional material and numerical parameters are listed in Tables III and IV.

The longitudinal bars were simulated as embedded elements into the brick elements. The external loads were applied in equal increments of 5 % of the expected failure load. These increments were reduced at stages close to the ultimate loads.

The numerical analyses have been generally carried out using the 27-point integration rule and a convergence tolerance of 2 %.

TABLE III: Material properties and additional material parameters of Ashour and Wafa beams.

$$E_c^* = 3320\sqrt{f'c} + 6900 \text{ for } 21 \text{ MPa} < f'_c < 81 \text{ MPa} \quad (10)$$

	B-4-0.0	***B-4-0.5***	***B-4-1.0***	***B-4-1.5***
Concrete				
Young's Modulus , E_c * (N/mm^2)	43600	43866	44117	44719
Compressive Strength , $f_{ć}$ (N/mm^2)	86.14	87.11	88.11	90.53
Tensile Strength , f_t (N/mm^2)	4.91	5.93	7.38	7.97
Poisson's Ratio, ν	0.2	0.2	0.2	0.2
Uniaxial Crushing Strain , ε_{cu}	0.003	0.0035	0.0038	0.004
Volumes Fraction of Fibers , V_f %	0.0	0.5	1.0	1.5
Aspect Ratio , L_f / d_f		75	75	75
Steel				
Young's Modulus , E_s (N/mm^2)	200000	200000	200000	200000
Longitudinal Bars				
Steel Ratio , ρ_w (%)	1.39	1.39	1.39	1.39
Yield Stress , f_y (N/mm^2)	437	437	437	437
Hardening Parameter H′	0.0	0.0	0.0	0.0
Stirrups				
Steel Ratio , ρ_v (%)	0.39	0.39	0.39	0.39
Yield Stress f_y	400	400	400	400
Hardening Parameter , H′	0.0	0.0	0.0	0.0
Tension-Stiffening Parameters				
Model	TS	TS1	TS1	TS1
α_1	90	125	130	200
α_2	0.6	0.7	0.8	0.9

TABLE IV: Material properties and additional material parameters of Ashour and Wafa beams.

	B-6-0.0	***B-6-0.5***	***B-6-1.0***	***B-6-1.5***
Concrete				
Young's Modulus , E_c * (N/mm^2)	43600	43866	44117	44719
Compressive Strength , $f_{ć}$ (N/mm^2)	86.14	87.11	88.11	90.50
Tensile Strength , f_t (N/mm^2)	4.91	5.93	7.38	7.97
Poisson's Ratio, ν	0.2	0.2	0.2	0.2
Uniaxial Crushing Strain , ε_{cu}	0.003	0.0035	0.0038	0.004
Volumes Fraction of Fibers , V_f %	0.0	0.5	1.0	1.5
Aspect Ratio , L_f / d_f		75	75	75
Steel				
Young's Modulus , E_s (N/mm^2)	200000	200000	200000	200000
Longitudinal Bars				
Steel Ratio , ρ_w (%)	1.39	1.39	1.39	1.39
Yield Stress , f_y (N/mm^2)	437	437	437	437
Hardening Parameter , H′	0.0	0.0	0.0	0.0
Stirrups				
Steel Ratio , ρ_v (%)	0.39	0.39	0.39	0.39
Yield Stress f_y	400	400	400	400
Hardening Parameter , H′	0.0	0.0	0.0	0.0
Tension-Stiffening Parameters				
Model	TS	TS1	TS1	TS1
α_1	90	125	130	200
α_2	0.6	0.7	0.8	0.9

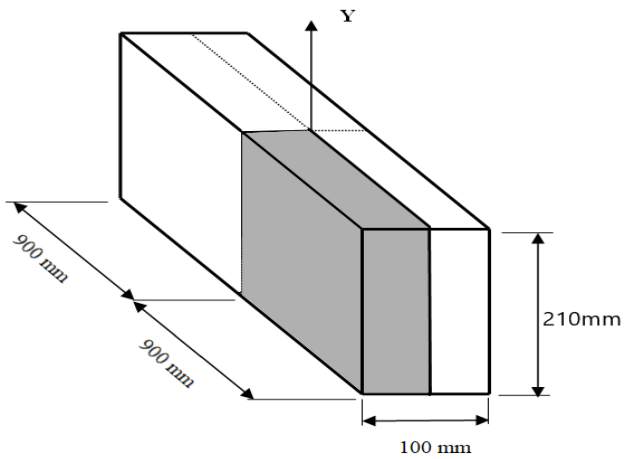

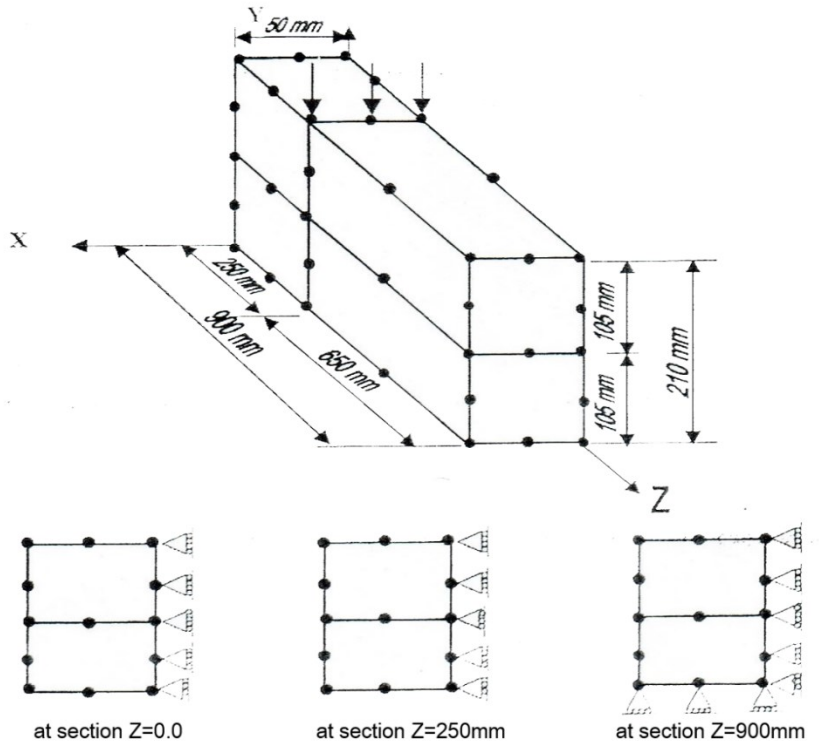

Figure 5: Finite element mesh and conditions for Ashour and Wafa beams [14].

5. RESULTS OF ANALYSIS

The experimental and numerical load – deflection curves for beams B4-0 to B6-1.5 are shown in Figures 6 and 7.

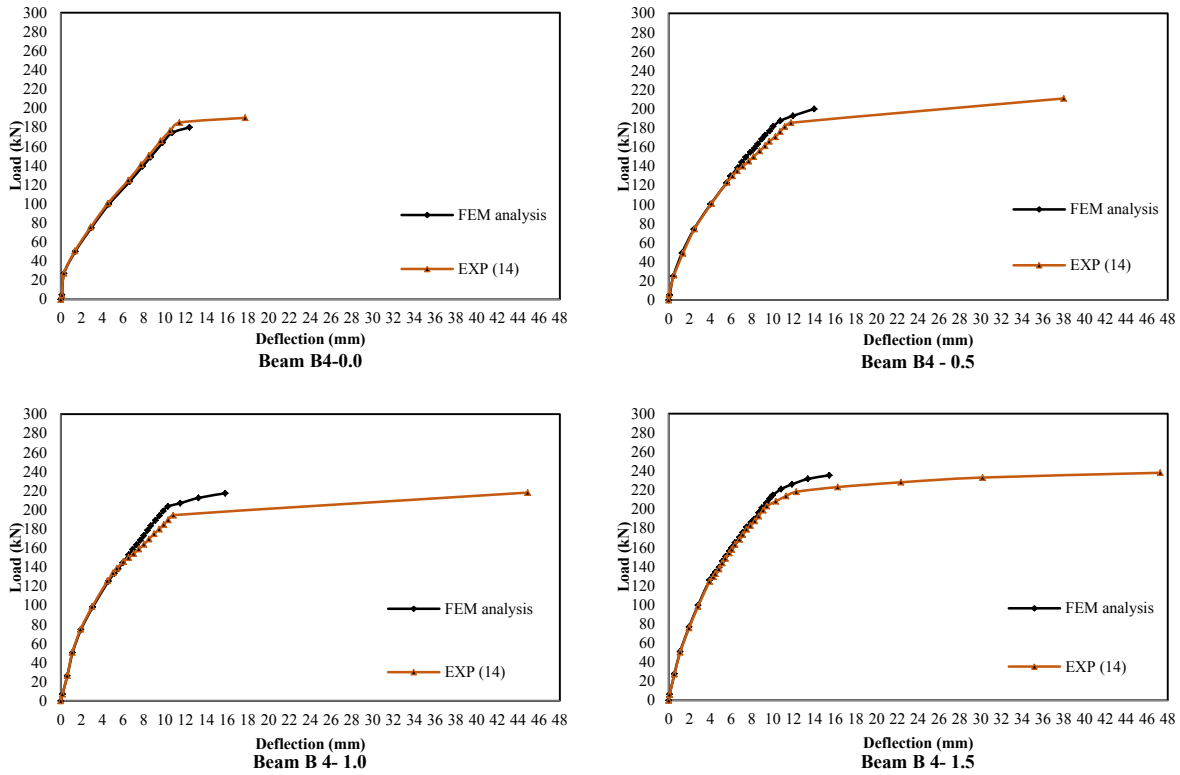

Figure 6: Beams B4 analytical and experimental load - deflection curves.

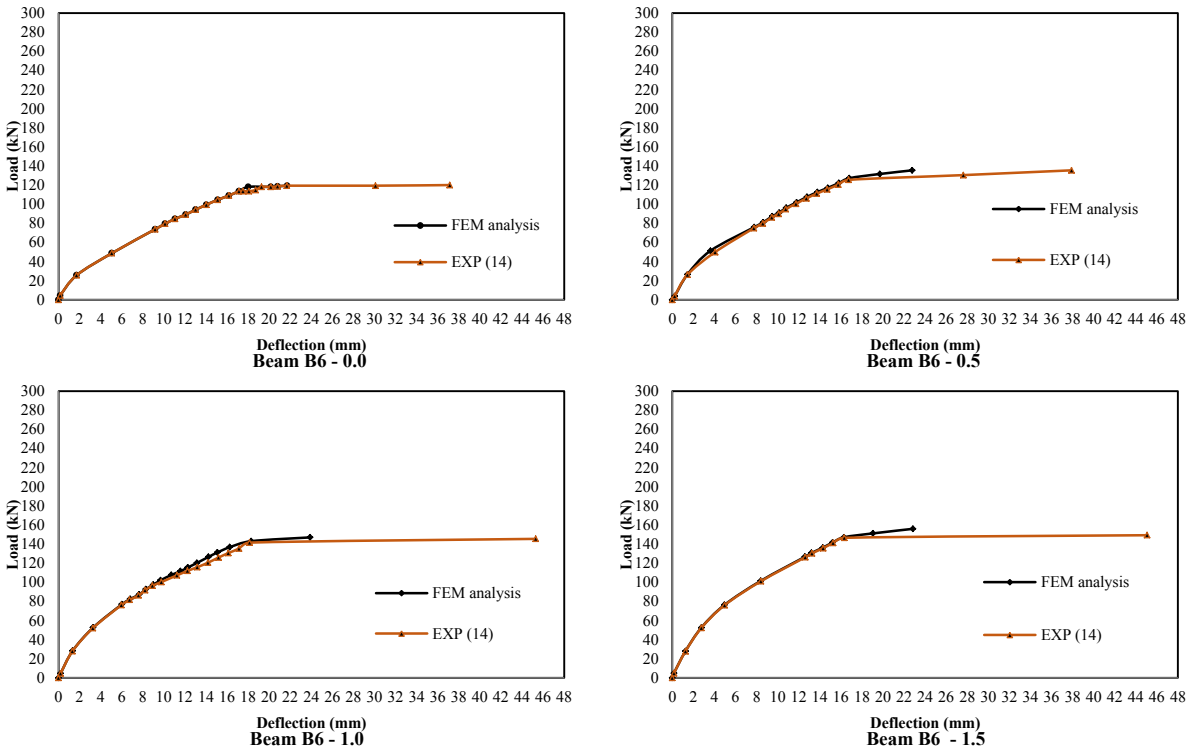

Figure7: Beams B6 analytical and experimental load – deflection curves.

These Figures show good agreement for the finite element solution compared with the experimental results throughout the entire range of behavior. They reveal that both the initial and post-cracking stiffnesses are reasonably predicted. The computed failure loads for all beams are close to the corresponding experimental collapse load as listed in Table V.

TABLE V: Comparison between experimental and predicted collapse loads.

Beams	*Experimental Collapse Load $P_{u,exp.}$ (kN)*	*Numerical Collapse Load (kN) $P_{u,num.}$*	$\frac{P_{u,num.}}{P_{u,exp.}}$
B4-0.0	190	180	0.947
B4-0.5	210	200	0.952
B4-1.0	220	220	1.0
B4-1.5	240	235	0.979
B6-0.0	122	122	1.0
B6-0.5	135	134	0.9926
B6-1.0	145	146	1.0069
B6-1.5	150	155	1.0333

6. PARAMETRIC STUDIES

To investigate the effects of some of the material and solution parameters on the nonlinear finite element analysis of high strength fiber concrete beams, beam B4-1 and B6-1 have been chosen to carry out a parametric study. This study helps to clarify the effect of various parameters that have been considered on the behavior and ultimate load capacity of the analyzed beams.

I. Influence of Fiber Content

The presence of fibers enhances the ductility and energy absorption capacity of reinforced concrete members and act as crack arresters. Therefore, the addition of a small amount of fibers can increase the flexural, shear and torsional capacity of the members.

To study the effect of using different amounts of fibers, six tests have been carried out with volume fraction of fiber ranging from 0.0 to 2.5%. Figure 8 shows that the post cracking stiffness and

the predicted cracking and ultimate load are considerably increased as the fiber content is increased. The finite element results revealed that an increase up to 54% and 51.6% in ultimate load capacity can be achieved by using a fiber content of 2.5% for beam B4-1 and B6-1 respectively as listed in Table VI.

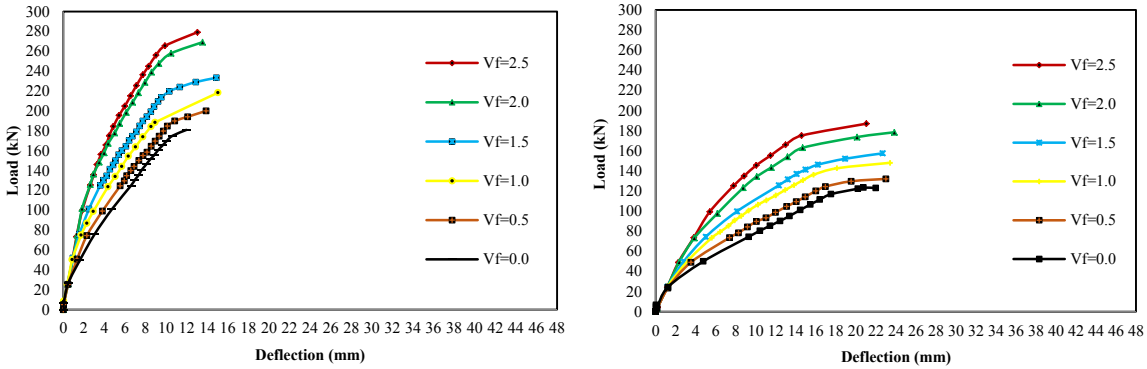

Figure 8: Influence of fiber content on load – deflection curve for beams B4, B6.

TABLE VI: Comparison between cracking and ultimate loads for different amount of fibers.

	V_f %	*Numerical Cracking Load (kN)*	*Numerical Ultimate Load (kN)*
B4	0.0	170	180
	0.5	185	200
	1.0	190	220
	1.5	215	235
	2.0	245	266
	2.5	265	277
B6	0.0	115	122
	0.5	125	134
	1.0	135	146
	1.5	145	155
	2.0	165	180
	2.5	175	185

II. Effect of Grade of Concrete

In the present research work, a study was made to investigate the use of concrete of higher compressive strength. This was achieved by numerically testing an assumed beam with a wide range of concrete compressive strength. This beam is similar in dimensions, arrangement of reinforcement and other details to B4-1 and B6-1. The tension stiffening parameters α_1 and α_2 were set equal to 130 and 0.8 respectively. While the shear retention parametersγ_1, $\gamma_2$and γ_3 were set equal to 10, 0.1 and 0.1 respectively.

The results of this investigation are shown in Figure 9. Three grades of concrete were considered in this study. These are 90,110 and 130 MPa the analysis revealed that the failure was due to yielding of reinforcement for all grades of concrete. Therefore the cracking load and post-cracking stiffness are increased slightly by increasing concrete compressive strength .The finite element results revealed that an increase up to 10% in ultimate load capacity can be achieved by using compressive strength equal to 130 MPa, compared to a compressive strength of 90 MPa for B4-1 and B6-1.

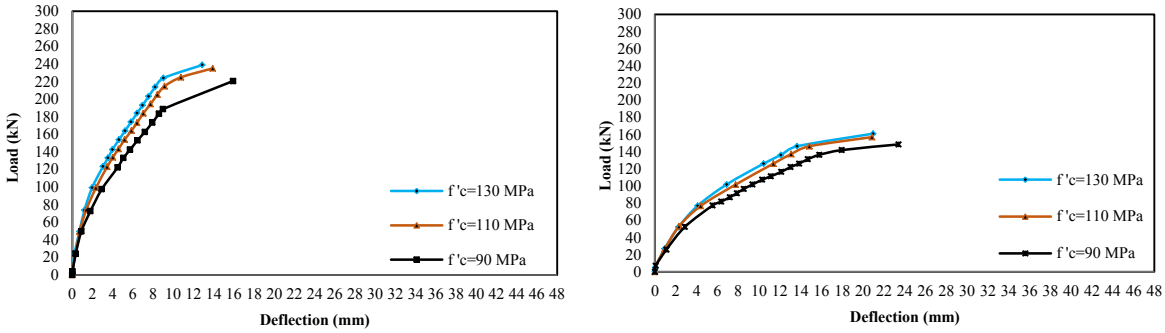

Figure 9: Influence of concrete grade on load – deflection curve for beams B 4-1.0 and B 6-1.0.

III. Influence of Longitudinal Reinforcement

The influence of using different longitudinal reinforcement ratios on the load- deflection curve is investigated. An assumed beam reinforced with various longitudinal reinforcement ratios was numerically tested. The results are shown in Figure 10. The longitudinal reinforcement ratio varied from 0.7 to 3.5%. The concrete compressive strength and reinforcement yield stress were 88.11 and 437 MPa respectively. By studying the predicted response of the beam, it can be seen that the increase in the longitudinal reinforcement ratio leads to a stiffer post-cracking response and significant increase in the ultimate load capacity of the beam. The finite element results revealed that an increase up to 153% in ultimate load capacity can be achieved by using longitudinal reinforcement ratio equal to 3.5%, compared to a ratio of 0.7% for B4-1 and B6-1 as listed in Table VII.

TABLE VII: Comparison between cracking and ultimate loads for different Longitudinal reinforcement ratio.

	ρ_w%	*Numerical Cracking Load (kN)*	*Numerical Ultimate Load (kN)*
	0.7	135	145
	1.4	190	220
B4	2.1	265	279
	2.8	325	338
	3.5	355	367
	0.7	90	95
	1.4	135	146
B6	2.1	175	186
	2.8	215	225
	3.5	235	251

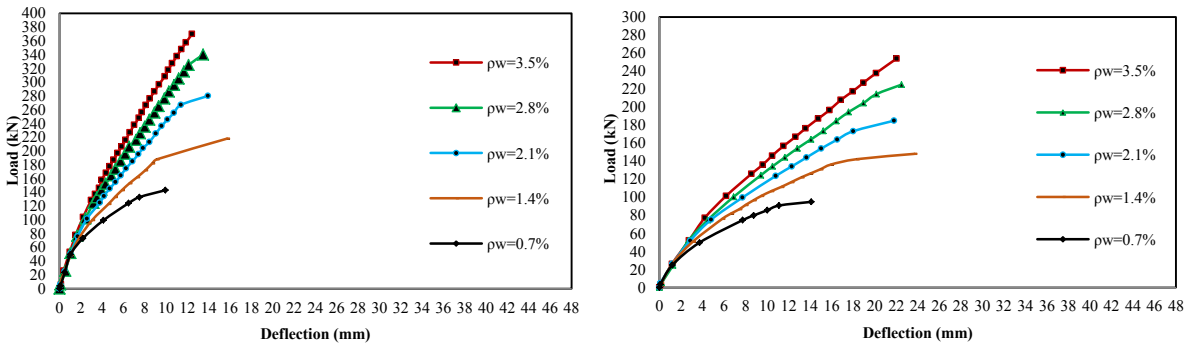

Figure 10: Influence of the longitudinal reinforcement ratio on load – deflection curve for beams B 4-1.0 and B 6-1.0.

7. CONCLUSIONS

The main conclusions of the theoretical work of this study can be summarized as follows:

1) The three dimensional nonlinear finite element model used in the present work is capable of simulating the behavior of fiber reinforced concrete beams subjected to monotonic loading. The finite element analysis carried out showed good agreement with the experimental results throughout the entire range of behavior.
2) The increase in concrete compressive strength results in a slightly increase in the ultimate load capacity of the beams when the failure is due to yielding of reinforcement.
3) The addition of a small amount of steel fibers to concrete significantly increases the cracking load. This may be attributed to crack arresting mechanism of fibers. An increase of 56% and 52% in cracking load can be achieved by using fiber content of 2.5% for beam B4-1 and B6-1 respectively.
4) The addition of steel fibers to concrete increases the collapse load. The value of the collapse load depends on the properties of fibers and type of failure. An increase of 54% and 51.6% in ultimate load capacity was obtained when a fiber content of 2.5% was added to beam B4-1 and B6-1 respectively.
5) The increase in longitudinal reinforcement ratio was found to increase ultimate load capacity and post-cracking stiffness. An increase up to 153% in ultimate load capacity can be achieved by using longitudinal reinforcement ratio of 3.5%.

REFERENCES

[1] L. J. Rasmussen, and G. Baker, "Torsion in Reinforced Normal and High-Strength Concrete Beams -Part1 Experimental Test Series," ACI Structural Journal, Jan-Feb. 1995, pp. 56-62.

[2] A. E. Naaman, and J. R. Homrich, "Properties of High-Strength Fiber Reinforced Concrete," ACI Publication, SP 87-13, 1985, pp.233-250.

[3] A. Y. Thannon, "Ultimate Load Analysis of Reinforced Concrete Stiffened Shells and Folded Slabs Used in Architectural Structures," Ph.D. Thesis, Univ. of Wales, Swansea, 1988.

[4] E. Hinton and D.R.J. Owen, "Finite Element Software for Plates and Shells," Pine ridge Press, Swansea, 1984.

[5] L. E. Allose, "Three Dimensional Nonlinear Finite Element Analysis of Steel Fiber Reinforced Concrete Beams in Torsion," M.Sc. Thesis, Univ. of Technology, Baghdad, Iraq, 1996.

[6] H.M.S. Abdul-Wahab, "Strength of reinforced concrete corbels with fibers," ACI Structure J., Vol.86, No.1, Jan., 1989, pp.60-66.

[7] F.J.Vecchio, M. P. Collins, and J. Aspiotis, "High Strength Concrete Elements Subjected to Shear," ACI Structural Journal, July-Aug. 1994, pp. 423-433.

[8] I.A.S. Al-Shaarbaf, "Three Dimensional Nonlinear Finite Element Analysis of Reinforced Concrete Beams in Torsion," Ph.D. Thesis, Univ. of Bradford, 1990.

[9] B. S. Al-Moussely, "Three Dimensional Nonlinear Finite Element Analysis for Steel Fiber Reinforced Concrete Beams Subjected to Combined Bending and Torsion," M.Sc. Thesis, Univ. of Technology, Baghdad, Iraq ,1998.

[10] J. H. Naji, and I. May, "The Effect of Some Numerical and Material Parameters on the Nonlinear Finite Element Analysis of Reinforced Concrete Beams," Proceedings of the Third Arab Engineering Conference, Vol. 1, March 1998, No. 5, pp. 10-17.

[11] Z. M. K. Al-Azzawi, "Capacity of High Strength Fiber Reinforced Beam Column Joints," M. Sc. Thesis, Univ. of Technology, Baghdad, Iraq, 1997.

[12] Z. J. Bunni, "Shear Strength in High-Strength Fiber Reinforced Concrete Beams," M. Sc. Thesis, Univ. of Technology, Baghdad, 1998, 105 PP.

[13] F. F. Wafa, and S. A. Ashour" Mechanical Properties of High Strength Fiber Reinforced Concrete, "ACI Materials Journal, Vol. 89, 1992, No. 5, pp. 455-499.

[14] S. A. Ashour, and F.F. Wafa, "Flexural Behavior of High-Strength Fiber Reinforced Concrete Beams, "ACI Structural Journal, Vol. 90 , No. 3 , May-June 1993 , pp. 279- 287.